Q-Save: Towards Scoring and Attribution for Generated Video Evaluation

Xiele Wu¹ Zicheng Zhang¹ Mingtao Chen^{3*} Yixian Liu³ Yiming Liu³ Shushi Wang¹ Zhichao Hu³ Yuhong Liu³ Guangtao Zhai¹ Xiaohong Liu^{1,2‡}

¹Shanghai Jiao Tong University ²Shanghai Innovation Institute ³Hunyuan, Tencent

Abstract

We present **Q-Save**, a new benchmark dataset and model for holistic and explainable evaluation of AI-generated video (AIGV) quality. The dataset contains near 10,000 videos, each annotated with a scalar mean opinion score (MOS) and fine-grained attribution labels along three core dimensions: visual quality, dynamic quality, and text-video alignment. These multi-aspect annotations enable both accurate quality assessment and interpretable reasoning behind the scores. To leverage this data, we propose a unified evaluation model that jointly performs quality scoring and attribution-based explanation. The model adopts the Slow-Fast framework to distinguish between fast frames and slow frames—slow frames are processed with high resolution while fast frames use low resolution, balancing evaluation accuracy and computational efficiency. For training, we use data formatted in Chain-of-Thought (COT) style and employ a multi-stage strategy: we first conduct Supervised Fine-Tuning (SFT), then further enhance the model with Grouped Relative Policy Optimization (GRPO), and finally perform SFT again to improve model stability. Experimental results demonstrate that our model achieves state-ofthe-art performance in video quality prediction while also providing human-aligned, interpretable justifications. Our dataset and model establish a strong foundation for explainable evaluation in generative video research, contributing to the development of multimodal generation and trustworthy AI. Code and dataset will be released upon publication.

1. Introduction

With the rapid advancement of generative AI, an increasing number of text-to-video (T2V) contents are being produced and disseminated through various platforms for both industrial applications and end-user consumption [19, 43]. However, due to current technological limitations, most T2V content still exhibits varying degrees of imperfec-

tion [27, 29, 32]. Consequently, there is a growing need for an automated evaluation framework that can assess the quality of generated videos effectively [8, 20, 21, 24, 32, 48–51, 53, 59, 61]. Such a framework can significantly reduce the cost of manual evaluation, improve the efficiency of video quality assessment, and serve as a critical tool in guiding the optimization of generative models.

To meet the need for evaluation, many text-to-vision evaluation datasets have been proposed, along with corresponding evaluation algorithms [5, 6, 12, 18, 23, 26– 28, 31, 35, 45, 55, 60, 63, 64]. However, these efforts face the following significant limitations: 1) The essential evaluation dimensions for text-to-vision content are typically not defined in a systematic manner. Some existing datasets introduce an excessive number of dimensions, which complicates the evaluation process without offering proportional benefits. Moreover, many of these dimensions tend to have limited practical relevance or exhibit significant overlap, resulting in redundancy. 2) The vast majority of existing datasets lack annotated attributive explanations for the assigned quality scores. While scalar scores alone have historically been used for training video assessment models, they are no longer sufficient for achieving high-quality evaluations in the context of complex, multimodal generative content. To advance the effectiveness and interpretability of video quality assessment models, it is imperative to develop a more structured dataset that includes both quantitative scores and corresponding explanatory annotations [65]. Such a dataset design can provide richer supervision signals and facilitate more nuanced model understanding. Therefore, we constructed a novel dataset in the following way.

Based on extensive theoretical and empirical analyses [35, 52, 53, 62, 65], we define three fundamental dimensions for evaluating text-to-video generation: **Visual Quality:** Refers to the perceptual quality of the video frames, including aspects such as detail fidelity, sharpness, and aesthetic appeal. **Dynamic Quality:** Captures the quality of temporal dynamics, assessing whether dynamic is smooth, coherent, and physically plausible. **Alignment with Text:** Measures the semantic alignment between the generated vi-

^{*} project leader.

[‡] Corresponding author.

A Bayern man with a crew cut sprints in a cycling race.







Please the describe the dynamic quality of the image in details. Legend

Irrelevant Reasoning Inaccurate Rating Accurate Rating

Qwen3-VL-8B-Instruct

The dynamic quality of this video is very high. The video captures the cyclist's movement in detail, with a clear focus on the cyclist's body and the surrounding environment. The lighting is bright and the colors are vibrant, which adds to the overall dynamic quality of the video. The video also has a sense of motion, with the cyclist's body and the surrounding environment moving in a fluid and natural way. Overall, the video is a great example of high-quality dynamic video production.



The motion quality of the video exhibits moderate issues. The main subject (cyclist) shows slight unnatural distortion in body proportions and movement, particularly noticeable in the leg pedaling motion and arm posture. The background elements, especially the spectators and distant scenery, have noticeable blurring and lack sharpness, which affects the overall visual quality.

Figure 1. Abilities of Q-Save-tuned Qwen3-VL-8B-Instruct on Score and Interpreter, in comparison with the baseline version.

sual content and the input text prompt, which can also be interpreted as generation accuracy. These dimensions comprehensively reflect both the perceptual and semantic aspects of video quality and provide a structured basis for evaluation.

From a human-centric perspective, video quality scoring is inherently intertwined with interpretability. According to the perception-decision integration framework, explanation and scoring are not independent, but rather components of a unified evaluation mechanism. Unlike conventional approaches that directly output numerical scores, large multimodal models (LMMs) are capable of understanding questions related to video quality and providing natural language justifications for their evaluations. This capability enables LMMs to offer more interpretable and transparent assessments.

Given this context, a key challenge arises: *How can we effectively train large language models (LLMs) to score with attribution data?* To this end, we constructed a dataset comprising both quality scores and corresponding human-written attributions. This dataset includes approximately 1,600 high-quality prompts. Using six of the best-performing open-source and proprietary models currently available, we generated a total of 9,600 videos. For annotation, we recruited 60 human raters who assessed the videos across the aforementioned three quality dimensions, providing both scores and natural language explanations. Each training video was annotated by three raters, while each

test video received annotations from twelve raters. In total, our dataset comprises: $8,000 \text{ videos} \times 3$ annotators \times 4 dimensions = 96, 000 ratings for training, 2,000 videos \times 12 annotators \times 4 dimensions = 96,000 ratings for testing, and nearly 40,000 natural language attribution explanations across the dataset. This comprehensive dataset lays the foundation for training LLMs to perform both quality scoring and interpretability-aware attribution, advancing the state of video quality evaluation in generative AI.

2. Related Work

2.1. Benchmarks for Text-to-Video Evaluation

Early benchmarks for text-to-vision tasks primarily relied on multimodal datasets annotated with textual captions [4, 16, 36]. However, as the importance of human feedback has gained increasing recognition, more recent benchmarks have shifted toward incorporating human-generated annotations [9, 17, 65]. Two commonly adopted annotation strategies are Side-by-Side (SBS) comparisons and Mean Opinion Score (MOS) ratings [37, 56]. SBS involves selecting the preferred sample from a pair, offering higher annotation consistency and reduced cognitive load for annotators. In contrast, MOS assigns an absolute score to a single instance, offering greater flexibility and broader applicability across diverse evaluation contexts [2, 25].

Evaluation dimensions in text-to-video tasks are generally grouped into three main categories [35, 62]: *visual quality, dynamic quality* and *text-visual alignment*. While

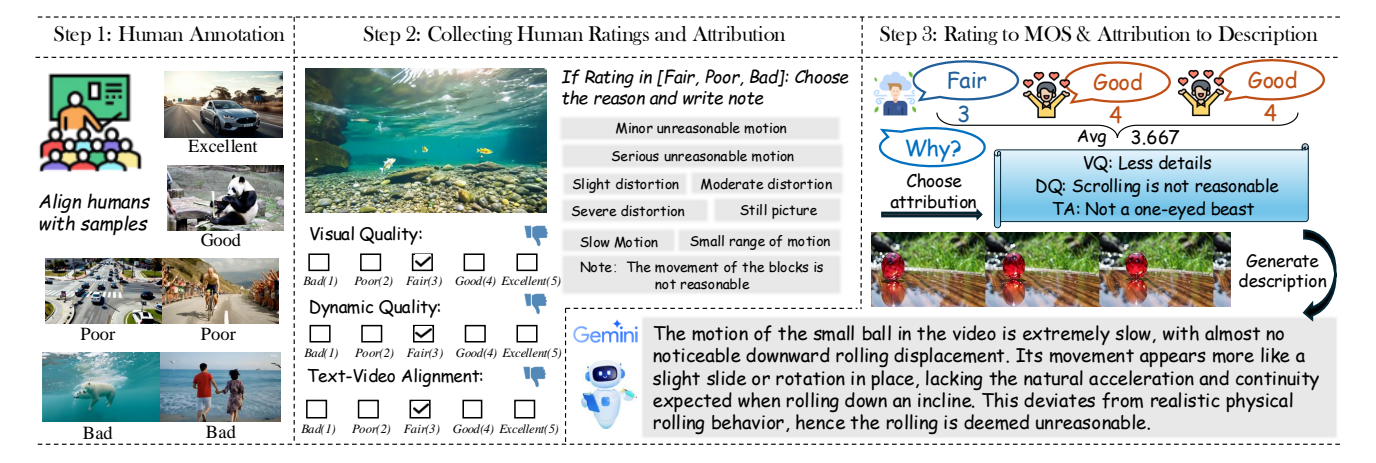


Figure 2. Human annotation process overview: 1) Raters are trained using text-defined rating levels; we simulate this with a rating-based syllabus for LMMs. 2) Raters assign scores and select reasons for low ratings (Bad–Fair). 3) Ratings are aggregated into MOS, and reasons are converted into descriptions; we propose a probability-based inference method for LMMs to generate final outputs.

some benchmarks [5, 6, 12, 18] define additional dimensions such as naturalness, aesthetics, and temporal coherence, we consider these subcomponents of the broader category of visual quality, as they collectively shape the viewer's Quality of Experience (QoE).

Early image generation benchmarks [27, 28, 45, 55] provided comprehensive evaluation protocols addressing both visual fidelity and semantic alignment. RichHF [31] further advanced this by integrating subjective ratings, visual heatmaps, and misalignment tokens to offer more detailed insights. In the video domain, VideoFeedback [12] introduces a five-dimensional assessment framework covering both quality and alignment, whereas T2VQA-DB [23]concentrates primarily on visual fidelity. Additionally, GenAI-Bench [26] provides alignment evaluations for both image and video generation.

In contrast to these efforts, the proposed Q-Save dataset establishes a unified framework for evaluating text-to-video content. It contributes to the development of video evaluation by building a new dataset structure.

2.2. Metric for Text-to-Video Evaluation

Previous evaluation approaches have predominantly treated visual quality, dynamic quality, and semantic alignment as separate concerns. **Visual quality** is typically assessed using perceptual metrics derived from pre-trained neural networks, such as Inception Score (IS) [38], Fréchet Inception Distance (FID) [15], and Learned Perceptual Image Patch Similarity (LPIPS) [58]. More recent work has introduced data-driven models [27] trained on curated perceptual datasets, enabling the prediction of visual quality through learned, domain-specific representations. These advances have contributed to more accurate assessments of spatial fidelity and artifact presence in generated content. Addi-

tionally, methods such as CLIP-IQA [44] and Q-Align [50] leverage text prompts to enhance perceptual alignment. Dynamic quality, referring to the temporal coherence and dynamic realism in videos, has historically been less emphasized in evaluation frameworks. Early metrics often failed to capture nuanced dynamic dynamics, relying instead on frame-based assessments that overlooked temporal artifacts[30, 39]. Recent research has started addressing this gap by incorporating motion-sensitive features and training evaluators on datasets with annotated dynamic quality [34], yet this area remains underexplored compared to static image assessment[57]. Alignment evaluation has evolved significantly, particularly with the introduction of CLIP-Score [14], which provided a simple yet effective measure of text-image correspondence. However, as prompts have become more diverse and semantically rich, alignment evaluation has increasingly relied on human feedback to capture subtleties not reflected in CLIP-based scores [21, 51, 53]. The emergence of large multimodal models (LMMs) with strong language-vision understanding has further enabled more nuanced assessments, leveraging their interpretive capabilities for complex prompt comprehension and matching [8, 20, 24, 32, 59].

Despite these advancements, most existing evaluation methods still treat visual quality, dynamic coherence, and alignment in isolation. The proposed *Q-Save* addresses this limitation by disentangling and simultaneously scoring all three dimensions, offering a comprehensive and interpretable evaluation framework for generative video models.

3. Data Construction

3.1. Basic Principles

The construction process of **Q-Save** is illustrated in Figure 4. Our dataset is constructed through a multi-stage pipeline

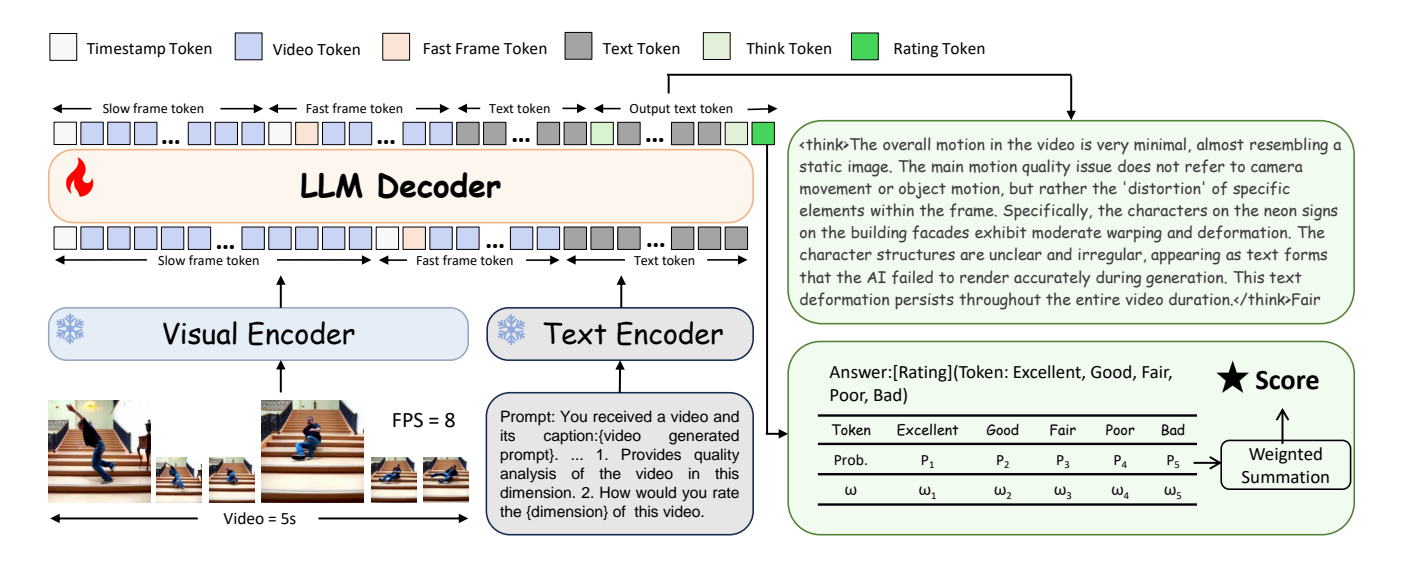


Figure 3. The model structure and video preprocessing. The model is based on the fine-tuned Qwen3-VL-8B-Instruct and adopts the SlowFast for video preprocessing to optimize the extraction of spatiotemporal features from videos (FPS = 8).

guided by three core principles: (1) **diversified prompt sources** coupled with the utilization of multiple generative models to enhance variety and robustness of the dataset and model; (2) **rigorous human quality control** to ensure the accuracy and reliability of annotations; and (3) **Contextaware adaptation** for LLMs: transforming scores and attribution explanations into a supervised fine-tuning (SFT) dataset to equip the model with interpretability—enabling it to understand the reasoning behind decisions—rather than merely memorizing data patterns. This approach ensures both breadth in data coverage and depth in model alignment. This structured methodology balances scalability with precision, making the dataset suitable for advanced language model training and evaluation.

3.2. Sources Collection

Prompt Collection. Most existing video datasets derive their prompts by sampling from various pre-existing sources or by filtering user-submitted content. However, such methods often result in a substantial number of low-quality prompts. In contrast, our prompts are manually authored to cover a comprehensive set of categories. This ensures not only complete category coverage but also guarantees that each prompt includes dynamic actions or camera movements. To further enhance quality and diversity, all prompts underwent multiple rounds of rewriting and manual review. As a result, our prompt set achieves a high degree of precision, richness, and diversity, making it well-suited for both training and evaluating generative video models.

Model Selection. We conducted a systematic evaluation of both open-source and proprietary video generation models

and selected six top-performing models based on preference rankings: Kling1.6 [41], Kling2.0 [41], Hunyuan [22], Veo2, Dreamina [3], and Wanx [10].

3.3. Subjective Experiment

Annotation Process. Given the critical importance of data quality for fine-tuning large language models, we implemented a rigorous annotation protocol to ensure the accuracy and reliability of labels. As illustrated in Figure 2, all annotators participated in a training program prior to formal annotation, aligning their understanding with our standards. This is followed by three rounds of pilot annotation. Annotators whose pilot results lacked sufficient accuracy received additional training to ensure full compliance with the annotation criteria. Once the formal annotation phase began, part of annotations underwent manual quality inspection. Annotations from individuals who continued to fall short of the required standards, especially regarding detailed completeness, were entirely excluded from the dataset.

The dataset was divided into training and testing sets with an 80:20 split. Each training instance was annotated by at least three annotators, while each test instance received annotations from no fewer than twelve annotators to ensure high reliability in quality assessment.

3.4. Data format

3.4.1. Context Prompt

Prior work on LMM-based evaluation often uses generic prompts lacking contextual grounding—for example, Q-Align [50]) asks "Can you evaluate the quality of the image?", while VQAScore [32] uses binary yes/no questions.

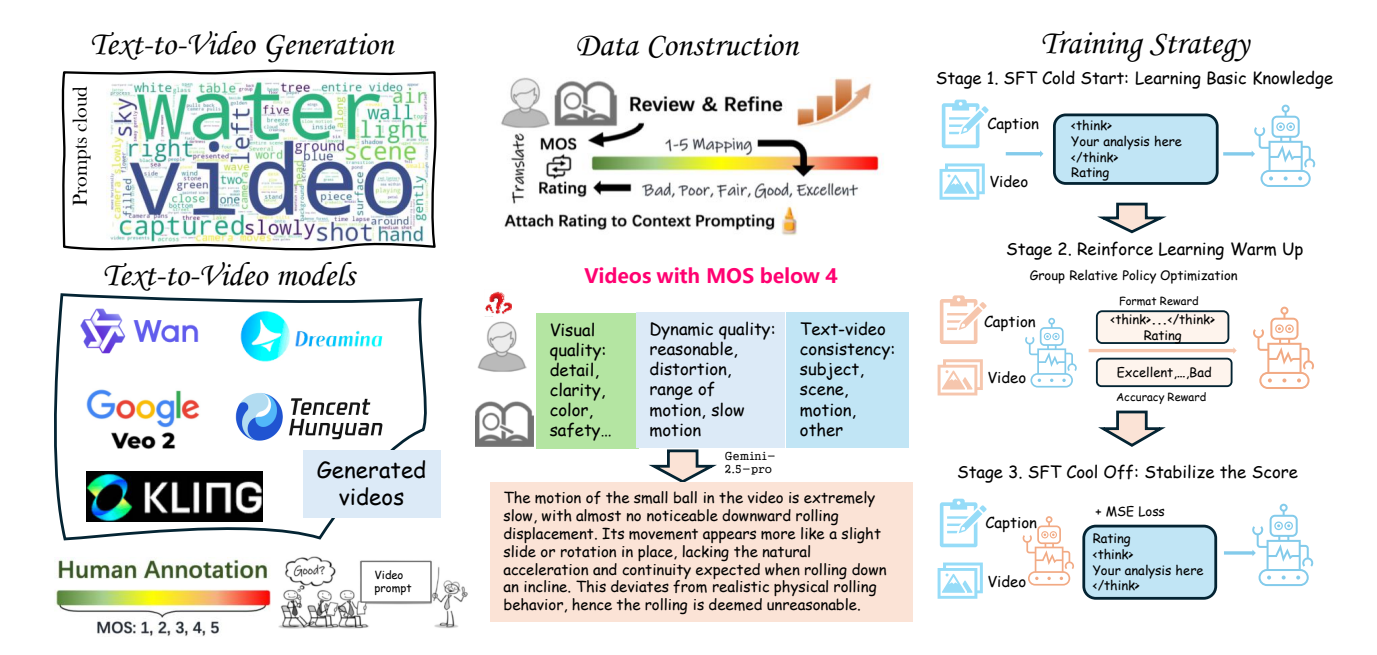


Figure 4. Overview of the Q-Save construction process and training strategy. We design prompts and employ models to generate videos. Subjective evaluations are then conducted to rate the quality of these generated instances. The resulting scores and descriptions constitute a dataset, and the corresponding knowledge is then injected into the linear mixed model according to the specified training strategy.

Such formulations are easy to implement but too vague for fine-grained or reliable evaluation, reducing interpretability and precision, especially in complex scenarios. To standardize the input format and enhance the model's comprehension ability during the training process, we have designed a specific Chain-of-Thought (COT) prompt template:

Judge its {dimension} based on following three criteria: {dimension criteria} . Considering the above video standards, you need to answer the following three questions: 1. Provides quality analysis of the video in this dimension. 2. How would you rate the visual quality of this video? Your rating can only be selected from the following five levels: [Bad, Poor, Fair, Good, Excellent]. Please integrate your answer with the following format: <think>Your analysis here</think>Rating

This open-ended structure encourages the model to provide rich, natural language explanations grounded in both the video content and its corresponding prompt.

3.4.2. "Translating" MOS into Ratings

It is well established that discrete adjective ratings are easier for LLMs to interpret compared to numerical scores [50, 61]. Since MOS in **Q-Save** is labeled in absolute terms, we can easily map MOS to the corresponding rating:

$$R(s) = r_i \quad \text{if} \quad m + \frac{i-1}{5}(M-m) < s \leq m + \frac{i}{5}(M-m),$$

where $\{r_i\}_{i=1}^5 = \{\text{Bad}, \text{Poor}, \text{Fair}, \text{Good}, \text{Excellent}\}, m =$

1 and M=5 (score range bound of **Q-Save**). R(s) indicates the mapped rating of MOS value s.

4. Q-Save

4.1. Unified Framework for Scoring and Attribution in Video Evaluation

Conventional methods often address video quality assessment and attribution as separate problems, relying on distinct models or modular pipelines. In this work, we introduce a unified framework that jointly performs *scoring* and *attribution* for AI-generated video content within a single model architecture. Our dataset is specifically constructed to support this joint formulation, providing both scalar mean opinion scores (MOS) and fine-grained attribution labels along three key dimensions.

This dual-supervision setup enables the model not only to deliver accurate quality predictions, but also to produce interpretable, dimension-specific explanations that reveal the underlying rationale for each assessment. Notably, we find that incorporating attribution signals during training improves not only the interpretability of model outputs but also enhances overall scoring accuracy. This demonstrates the synergistic effect of combining evaluation and explanation, and highlights the potential of attribution-guided learning in building more robust and trustworthy video quality evaluators.

Table 1. Performance com	nparison on the Visua	al quality, Dynamin	c quality and Alignment o	of Q-Save. Best in bol	d , second underlined.
			1 2		

	Visual Quality		Dynamic Quality				Alignment					
Model	Instanc	ce-level	Mode	l-level	Instanc	e-level	Mode	l-level	Instand	ce-level	Mode	l-level
	SRCC	PLCC	SRCC	PLCC	SRCC	PLCC	SRCC	PLCC	SRCC	PLCC	SRCC	PLCC
FastVQA	0.087	0.062	-0.103	-0.091	0.125	0.073	-0.542	-0.376	0.294	0.271	0.513	0.432
SimpleVQA	0.152	0.119	-0.076	-0.048	0.193	0.138	0.089	0.021	0.316	0.295	0.547	0.479
Dover	0.238	0.214	0.169	0.157	0.286	0.263	0.227	0.201	0.352	0.334	0.569	0.513
Q-Align	0.275	0.253	0.198	0.184	0.312	0.291	0.254	0.232	0.378	0.359	0.583	0.536
VisionReward	0.302	0.281	0.231	0.217	0.345	0.324	0.286	0.265	0.394	0.376	0.597	0.554
UnifiedReward	0.432	0.415	0.582	0.567	0.428	0.409	0.526	0.513	0.435	0.418	0.668	0.654
VideoScore-v2	0.397	0.381	0.613	0.592	0.395	0.378	0.498	0.482	0.447	0.429	0.643	0.627
Q-Save	0.634	0.650	1.000	0.910	0.679	0.672	0.943	0.865	0.701	0.707	1.000	0.970

4.2. Model Architecture

We select Qwen-VL [1] as the LMM model (Qwen3-VL-8B-Instruct) for training, which has demonstrated strong visual understanding capabilities for videos. As shown in Figure 3, we have made certain modifications to the video preprocessing method, scoring approach, and training loss.

4.2.1. Video Processing

For video encoding with varying FPS, resolutions, and durations, linearly increasing any of these factors leads to a sharp surge in the token budget on the LLM side—posing significant challenges to balancing performance and cost. To our knowledge, most existing MLLMs typically adopt a fixed number of frames and correspondingly reduce the resolution of each frame to comply with token budget constraints. Nevertheless, under a uniform frame sampling strategy, even though many adjacent frames may be highly similar, there remain cases where consecutive frames exhibit substantial differences. This is particularly true when the sampling interval is larger, or when a person is moving or the viewpoint is shifting. As a result, the simplistic 2D convolution merging technique may hinder effective video understanding, as it relies on overly strong assumptions. Considering the inherent characteristics of videos—where adjacent frames are mostly similar yet occasionally exhibit significant changes—we employ a SlowFast video encoding strategy [42]:

Slow Pathway: This pathway is designed to capture visual information from rapidly changing frames. It operates with a smaller number of frames but at a higher resolution.

Fast Pathway: In contrast, the Fast Pathway captures subtle changes in visual signals from relatively static frames. It uses a larger number of frames but at a lower resolution.

To identify slow/fast frames from a video, we first develop a patch-based similarity function for frame classification: (1) The first frame is always designated as a slow frame; (2) For each subsequent frame, if its patch similarity with the most recent slow frame exceeds 90%, it is labeled as a fast frame; otherwise, it is marked as a new slow frame. Additionally, to more clearly delineate the boundaries and

timestamp information between Slow and Fast frames, we introduce extra special tokens along with absolute timestamps to guide the model during training.

4.2.2. Scoring Method

The scoring calculation method is detailed below. First, we find the raing token, and then calculate the model output probability p_j for each of the five scoring items. $\{Excellent, Good, Fair, Poor, Bad\}$, where $j \in \{1, 2, 3, 4, 5\}$. Then we define the final predicted rating \hat{r} as the weighted average of these probabilities:

$$\hat{r} = \sum_{j=1}^{5} p_j \cdot w_j,$$

where w_j is the numerical weight assigned to each rating (e.g., $w_j = \{1, 0.75, 0.5, 0.25, 0\}$ for Excellent to Bad).

4.2.3. Loss function

The loss function of the model consists of two components: Cross-Entropy (CE) Loss and Mean Squared Error (MSE) Loss, The total loss is a weighted sum of the two.

The CE Loss helps the LMM learn the general questionanswer format, defined as:

$$\mathcal{L}_{CE} = -\sum_{i=1}^{N} y_i \cdot \log(p_i),$$

where y_i is the encoded vector of the true label for instance i, and p_i is the predicted probability vector for the answer tokens. The MSE Loss refines the score prediction accuracy, given by:

$$\mathcal{L}_{MSE} = \left(\hat{r} - r_{MOS}\right)^2,$$

where \hat{r} and r_{MOS} are the predicted score and the MOS label, respectively. The total loss is a weighted sum of the two:

$$\mathcal{L} = \alpha_1 \cdot \mathcal{L}_{CE} + \beta_1 \cdot \mathcal{L}_{MSE},$$

with α_1 and β_1 (default 1 and 1) controlling the contribution of each term.

Table 2. Cross-dataset validation performance on out-of-domain Benchmarks: 3 pairwise preference benchmarks and 2 point-score bench-
marks. Bold denotes the best model, <u>underlined</u> denotes the second best, and "/" denotes the method trained on the homologous training
set of the benchmark (not involved in comparison).

	OOD Pr	eferrence Bend	hmark	00	OD Point Scor	e Benchmark	
Method	VideoGen-	GenAI	T2VQADB	VideoPhy2	Vid	eoScore-Bencl	n-v2
	RewardBench	Bench	Preference	-test	Visual	Align	Phy
VideoReward	/	72.89	36.15	31.33	46.36	48.31	35.23
VisionReward	54.31	73.30	37.64	22.58	46.85	45.32	38.25
Q-Align	42.05	64.25	43.24	23.22	54.71	34.01	37.78
AIGVE-MACS	37.09	53.21	36.91	16.93	27.30	6.90	13.03
VideoPhy2	30.75	51.50	24.12	37.64	25.50	35.42	25.41
Dover	54.27	62.40	44.62	28.21	50.24	32.83	33.00
VideoScore-v2	51.53	75.80	50.60	33.58	/	/	/
Q-Save	56.88	<u>74.20</u>	59.45	41.18	<u>49.25</u>	58.70	38.57

4.3. Training Strategy

SFT Cold Start. We propose a three-stage training strategy for Q-Save. To ensure basic format-following ability and task familiarity, we first perform supervised fine-tuning (SFT) as the cold-start.

RL Warm Up. We further train the SFT checkpoint using Generative Ranked Policy Optimization (GRPO) implemented via the open-source video reinforcement learning framework Verl [40], with data from another smaller video dataset we constructed. Details of this dataset are provided in Appendix A.1.

Accuracy Reward. The accuracy reward is designed to directly guide the model to learn precise matching between its output and the true discrete labels of video reasoning tasks. The reward is determined by the degree of matching, and the design principle of this reward signal is as follows: it is assigned a value of 1 if it matches the true discrete label in this dimension, and 0 if there is a mismatch. The formal definition is as follows:

$$R_{\rm acc} = \begin{cases} 1.0 & \text{if match exactly,} \\ 0 & \text{otherwise.} \end{cases}$$

Format Reward. To ensure the output includes both a rationale and final scores, we assign $R_{fmt}=1$ if the response contains the <think> tag with rationale, and $R_{fmt}=0$ otherwise.

Final Reward. Following the setting for general video reasoning tasks in Video-R1 [11], final reward $R = R_{acc} + \lambda R_{fmt}$, where $\lambda = 0.5$.

RL training uses a batch size of 256, a learning rate of 2e-6, with G = 8 generations per rollout on $16 \times H20$ GPUs (about 1 hour per step).

SFT Cool Off. We saved the correct data rolled out in the second stage (reinforcement learning, RL), reformat it into the structure of "Rating<think>...reason...</think>", and then perform Supervised Fine-Tuning (SFT) again on this reformatted data. The rationale is that the RL-refined model

exhibits instability in video quality evaluation due to its CoT structure, whereas the model trained on the aforementioned reformatted data produces stable scores under our scoring method.

5. Experiment

5.1. Experiment Setup

Training & Evaluation. We employed **Qwen3-VL-8B-Instruct** [1] as the backbone large language model (LLM) throughout the training process, which was conducted in two distinct stages using a cluster of 8 NVIDIA H20 GPUs.

For evaluation metrics, we use SRCC and PLCC, which measure the rank and linear cor- relation between predicted scores and MOSs. We use evaluations at the **Instance-level** and **Model-level** which assess accuracy in ranking specific generated instances and generative models.

Competitors. We select representative video quality assessment and visual reward model competitors covering different technical paradigms. We include FastVQA [34], SimpleVQA [7], Q-Align [50], Dover [47], VideoScorev2 [13], UnifiedReward [46], VideoReward [33], and VisionReward [54].

All models are evaluated using their publicly available implementations, recommended hyperparameters, and the corresponding splits of the Q-Save dataset unless otherwise specified.

5.2. Discussion & General Findings

The performance comparison across visual, dynamic, and alignment is presented in Table 1. The results reveal the following:1) Visual Quality. Q-Save outperforms all baselines comprehensively across both instance- and modellevel evaluations. At the instance level, it achieves the highest SRCC (0.634) and PLCC (0.650), significantly surpassing the second-best method UnifiedReward. At the model level, it attains a perfect SRCC of 1.000 and a leading PLCC of 0.910, outperforming the second-ranked VideoScore-v2.

Table 3. Ablation study on training strategies.	We report SRCC and PLCC for visual quality, dynamic quality, alignment, and overall
quality at both instance-level and model-level. I	Multi-stage training achieves the best performance across all evaluation dimensions.

		Visual	Quality			Dynamic	Quality			Align	ment	
Strategy	Instance-level Model-level		Instanc	Instance-level Model-level		Instance-level		Model-level				
	SRCC	PLCC	SRCC	PLCC	SRCC	PLCC	SRCC	PLCC	SRCC	PLCC	SRCC	PLCC
Stage 1 w/o slowfast	0.50	0.51	0.58	0.57	0.58	0.57	0.54	0.58	0.63	0.61	0.79	0.75
Stage 1	0.57	0.54	0.61	0.60	0.61	0.60	0.52	0.51	0.66	0.65	0.84	0.81
Stage 1+2	<u>0.61</u>	<u>0.60</u>	0.71	0.63	0.64	0.63	0.74	0.65	<u>0.67</u>	0.66	0.87	0.86
Stage 1+2+3	0.63	0.65	1.00	0.91	0.68	0.67	0.94	0.86	0.70	0.70	1.00	0.97

2) Dynamic Quality. Q-Save maintains dominant performance in dynamic quality assessment. For instance-level metrics, it achieves the highest SRCC (0.679) and PLCC (0.672), far exceeding the second-best UnifiedReward. At the model level, it delivers an outstanding SRCC of 0.943 and PLCC of 0.865, outperforming UnifiedReward, which ranks second. 3) Text-Video Alignment. Q-Save surpasses all baseline alignment models by a notable margin. It achieves the highest instance-level SRCC (0.701) and PLCC (0.707), outperforming the second-best VideoScorev2. At the model level, it attains a perfect SRCC of 1.000 and an exceptional PLCC of 0.970, exceeding the secondranked UnifiedReward. 4) Interpretability. While perceptual quality remains inherently subjective—especially for visual quality—Q-Save maintains strong performance and interpretability. Its alignment evaluation benefits from grounded language-vision correspondence, further supporting its utility as a comprehensive and explainable metric for fine-grained AIGV assessment.

Cross-dataset Validation. To demonstrate the generalization capability of our Q-Save model and the value of its training paradigm, we conduct cross-dataset validations on out-of-domain (OOD) benchmarks, including 3 pairwise preference benchmarks and 2 point-score benchmarks, with results summarized in Table 2. On the OOD preference benchmarks, our Q-Save model achieves the best performance on T2VQADB Preference with a score of 59.45, significantly outperforming existing methods such as VideoScore-v2 (50.60). It also ranks first on VideoGen-RewardBench with a score of 56.88, surpassing the secondbest model VisionReward (54.31), and achieves the secondbest performance on GenAI Bench with 74.20, only slightly behind the top-performing VideoScore-v2 (75.80). For the OOD point-score benchmarks, Q-Save stands out on VideoPhy2-test with an impressive score of 41.18, which is substantially higher than the second-best model Video-Phy2 (37.64). On VideoScore-Bench-v2, it exhibits exceptional alignment capability with the best score of 58.70, and also achieves the second-best performance on the Phy metric (38.57) and a competitive second-best score on the Visual metric (49.25) behind Q-Align (54.71). Collectively, these results not only validate that our Q-Save model can

generalize robustly to unseen datasets across different evaluation paradigms but also highlight the effectiveness of our approach in learning transferable reward signals, further underscoring the practical value of our model for real-world video generation evaluation tasks.

5.3. Ablation Study

To dissect the efficacy of our multi-stage training strategy—SFT cold-start (with/without slowfast preprocessing), GRPO-based RL warm-up, and SFT cool-off-we conduct ablation experiments (Table 3). Stage 1 (SFT) without slowfast achieves instance-level SRCCs of 0.50 (visual), 0.58 (dynamic), 0.63 (alignment); with slowfast, these rise to 0.57, 0.61, 0.66, demonstrating that slowfast enhances the model's initial ability to capture video temporal-spatial features. Stage 1+2 (RL warm-up) shows substantial gains, reaching SRCCs of 0.61, 0.64, 0.67 (instance-level) and 0.71, 0.74, 0.87 (model-level). This confirms that GRPO effectively boosts the model's analytical robustness and alignment with human subjective judgments by optimizing reward signal learning. Stage 1+2+3 (SFT cool-off) attains best performance, with bold SRCCs of 0.63, 0.68, 0.70 (instance-level) and 1.00, 0.94, 1.00 (model-level), plus bold PLCCs of 0.91, 0.86, 0.97. These results validate that the final SFT cool-off stage mitigates the training instability introduced by CoT while preserving and refining the reward signals learned during warm-up. This confirms the final SFT mitigates RL instability while refining rewards, validating our strategy's role in unlocking the model's full potential for accurate quality scoring.

6. Conclusion

In this paper, we introduce **Q-Save**, a large-scale, diverse dataset tailored for evaluating and explaining the quality of AI-generated videos (AIGVs). It comprises 10,000 videos spanning real-world scenes, animations, and abstract content, each annotated with precise scalar scores and fine-grained attribution rationales across three dimensions. Building on Q-Save, we propose a unified evaluation model that excels at both accurate quality scoring and interpretable attribution-based explanation. Integrating the "slowfast" concept—capturing both fine details and

dynamic motion—and a multi-stage training strategy, our model achieves the best overall performance. This framework establishes a new benchmark for explainable AIGV quality evaluation, advancing research in multimodal reasoning and interpretable generative model assessment.

References

- [1] Jinze Bai, Shuai Bai, Shusheng Yang, Shijie Wang, Sinan Tan, Peng Wang, Junyang Lin, Chang Zhou, and Jingren Zhou. Qwen-vl: A versatile vision-language model for understanding, localization, text reading, and beyond. *arXiv* preprint arXiv:2308.12966, 2023. 6, 7
- [2] Shane Barratt and Rishi Sharma. A note on the inception score. *arXiv preprint arXiv:1801.01973*, 2018. 2
- [3] Dreamina by CapCut. Dreamina, 2023. Available online at https://dreamina.capcut.com/. 4
- [4] Xinlei Chen, Hao Fang, Tsung-Yi Lin, Ramakrishna Vedantam, Saurabh Gupta, Piotr Dollár, and C Lawrence Zitnick. Microsoft COCO captions: Data collection and evaluation server. CoRR, abs/1504.00325, 2015.
- [5] Zijian Chen, Wei Sun, Haoning Wu, Zicheng Zhang, Jun Jia, Xiongkuo Min, Guangtao Zhai, and Wenjun Zhang. Exploring the naturalness of ai-generated images. arXiv preprint arXiv:2312.05476, 2023. 1, 3
- [6] Zijian Chen, Wei Sun, Yuan Tian, Jun Jia, Zicheng Zhang, Jiarui Wang, Ru Huang, Xiongkuo Min, Guangtao Zhai, and Wenjun Zhang. Gaia: Rethinking action quality assessment for ai-generated videos. arXiv preprint arXiv:2406.06087, 2024. 1, 3
- [7] Xianfu Cheng, Wei Zhang, Shiwei Zhang, Jian Yang, Xiangyuan Guan, Xianjie Wu, Xiang Li, Ge Zhang, Jiaheng Liu, Yuying Mai, Yutao Zeng, Zhoufutu Wen, Ke Jin, Baorui Wang, Weixiao Zhou, Yunhong Lu, Tongliang Li, Wenhao Huang, and Zhoujun Li. Simplevqa: Multimodal factuality evaluation for multimodal large language models, 2025.
- [8] Jaemin Cho, Yushi Hu, Roopal Garg, Peter Anderson, Ranjay Krishna, Jason Baldridge, Mohit Bansal, Jordi Pont-Tuset, and Su Wang. Davidsonian scene graph: Improving reliability in fine-grained evaluation for text-image generation. arXiv preprint arXiv:2310.18235, 2023. 1, 3
- [9] Paul F Christiano, Jan Leike, Tom Brown, Miljan Martic, Shane Legg, and Dario Amodei. Deep reinforcement learning from human preferences. Advances in neural information processing systems, 30, 2017. 2
- [10] Alibaba Cloud. Wanx. https://tongyi.aliyun. com/wanxiang/, 2024. Accessed: 2024-11-07. 4
- [11] Kaituo Feng, Kaixiong Gong, Bohao Li, Zonghao Guo, Yibing Wang, Tianshuo Peng, Junfei Wu, Xiaoying Zhang, Benyou Wang, and Xiangyu Yue. Video-r1: Reinforcing video reasoning in mllms, 2025. 7
- [12] Xuan He, Dongfu Jiang, Ge Zhang, Max Ku, Achint Soni, Sherman Siu, Haonan Chen, Abhranil Chandra, Ziyan Jiang, Aaran Arulraj, Kai Wang, Quy Duc Do, Yuansheng Ni, Bohan Lyu, Yaswanth Narsupalli, Rongqi Fan, Zhiheng Lyu, Yuchen Lin, and Wenhu Chen. Videoscore: Building automatic metrics to simulate fine-grained human feedback for video generation. *ArXiv*, abs/2406.15252, 2024. 1, 3

- [13] Xuan He, Dongfu Jiang, Ping Nie, Minghao Liu, Zhengxuan Jiang, Mingyi Su, Wentao Ma, Junru Lin, Chun Ye, Yi Lu, Keming Wu, Benjamin Schneider, Quy Duc Do, Zhuofeng Li, Yiming Jia, Yuxuan Zhang, Guo Cheng, Haozhe Wang, Wangchunshu Zhou, Qunshu Lin, Yuanxing Zhang, Ge Zhang, Wenhao Huang, and Wenhu Chen. Videoscore2: Think before you score in generative video evaluation, 2025.
- [14] Jack Hessel, Ari Holtzman, Maxwell Forbes, Ronan Le Bras, and Yejin Choi. Clipscore: A reference-free evaluation metric for image captioning. arXiv preprint arXiv:2104.08718, 2021. 3
- [15] Martin Heusel, Hubert Ramsauer, Thomas Unterthiner, Bernhard Nessler, and Sepp Hochreiter. Gans trained by a two time-scale update rule converge to a local nash equilibrium. In Advances in neural information processing systems, pages 6626–6637, 2017. 3
- [16] Yushi Hu, Benlin Liu, Jungo Kasai, Yizhong Wang, Mari Ostendorf, Ranjay Krishna, and Noah A Smith. Tifa: Accurate and interpretable text-to-image faithfulness evaluation with question answering. In *Proceedings of the IEEE/CVF International Conference on Computer Vision*, pages 20406–20417, 2023. 2
- [17] Kaiyi Huang, Kaiyue Sun, Enze Xie, Zhenguo Li, and Xihui Liu. T2i-compbench: A comprehensive benchmark for open-world compositional text-to-image generation. Advances in Neural Information Processing Systems, 36:78723-78747, 2023. 2
- [18] Ziqi Huang, Yinan He, Jiashuo Yu, Fan Zhang, Chenyang Si, Yuming Jiang, Yuanhan Zhang, Tianxing Wu, Qingyang Jin, Nattapol Chanpaisit, et al. Vbench: Comprehensive benchmark suite for video generative models. In *Proceedings of* the IEEE/CVF Conference on Computer Vision and Pattern Recognition, pages 21807–21818, 2024. 1, 3
- [19] Everypixel Journal. Ai image statistics for 2024: How much content was created by ai. *Everypixel*, 2024. Accessed: 2024-10-14. 1
- [20] Seungone Kim, Jamin Shin, Yejin Cho, Joel Jang, Shayne Longpre, Hwaran Lee, Sangdoo Yun, Seongjin Shin, Sungdong Kim, James Thorne, et al. Prometheus: Inducing finegrained evaluation capability in language models. arXiv preprint arXiv:2310.08491, 2023. 1, 3
- [21] Yuval Kirstain, Adam Polyak, Uriel Singer, Shahbuland Matiana, Joe Penna, and Omer Levy. Pick-a-pic: An open dataset of user preferences for text-to-image generation. *Advances in Neural Information Processing Systems*, 36: 36652–36663, 2023. 1, 3
- [22] Weijie Kong, Qi Tian, Zijian Zhang, Rox Min, Zuozhuo Dai, Jin Zhou, Jiangfeng Xiong, Xin Li, Bo Wu, Jianwei Zhang, Kathrina Wu, Qin Lin, Junkun Yuan, Yanxin Long, Aladdin Wang, Andong Wang, Changlin Li, Duojun Huang, Fang Yang, Hao Tan, Hongmei Wang, Jacob Song, Jiawang Bai, Jianbing Wu, Jinbao Xue, Joey Wang, Kai Wang, Mengyang Liu, Pengyu Li, Shuai Li, Weiyan Wang, Wenqing Yu, Xinchi Deng, Yang Li, Yi Chen, Yutao Cui, Yuanbo Peng, Zhentao Yu, Zhiyu He, Zhiyong Xu, Zixiang Zhou, Zunnan Xu, Yangyu Tao, Qinglin Lu, Songtao Liu, Dax Zhou, Hongfa Wang, Yong Yang, Di Wang, Yuhong Liu, Jie Jiang,

- and Caesar Zhong. Hunyuanvideo: A systematic framework for large video generative models, 2025. 4
- [23] Tengchuan Kou, Xiaohong Liu, Zicheng Zhang, Chunyi Li, Haoning Wu, Xiongkuo Min, Guangtao Zhai, and Ning Liu. Subjective-aligned dateset and metric for text-to-video quality assessment. arXiv preprint arXiv:2403.11956, 2024. 1,
- [24] Max Ku, Dongfu Jiang, Cong Wei, Xiang Yue, and Wenhu Chen. Viescore: Towards explainable metrics for conditional image synthesis evaluation. arXiv preprint arXiv:2312.14867, 2023. 1, 3
- [25] Lucie Lévêque, Meriem Outtas, Hantao Liu, and Lu Zhang. Comparative study of the methodologies used for subjective medical image quality assessment. *Physics in Medicine & Biology*, 66(15):15TR02, 2021.
- [26] Baiqi Li, Zhiqiu Lin, Deepak Pathak, Jiayao Li, Yixin Fei, Kewen Wu, Tiffany Ling, Xide Xia, Pengchuan Zhang, Graham Neubig, et al. Genai-bench: Evaluating and improving compositional text-to-visual generation. arXiv preprint arXiv:2406.13743, 2024. 1, 3
- [27] Chunyi Li, Zicheng Zhang, Haoning Wu, Wei Sun, Xiongkuo Min, Xiaohong Liu, Guangtao Zhai, and Weisi Lin. AGIQA-3K: An open database for ai-generated image quality assessment. *CoRR*, 2306.04717, 2023. 1, 3
- [28] Chunyi Li, Tengchuan Kou, Yixuan Gao, Yuqin Cao, Wei Sun, Zicheng Zhang, Yingjie Zhou, Zhichao Zhang, Weixia Zhang, Haoning Wu, et al. Aigiqa-20k: A large database for ai-generated image quality assessment. *arXiv preprint arXiv:2404.03407*, 2(3):5, 2024. 1, 3
- [29] Chunyi Li, Haoning Wu, Zicheng Zhang, Hongkun Hao, Kaiwei Zhang, Lei Bai, Xiaohong Liu, Xiongkuo Min, Weisi Lin, and Guangtao Zhai. Q-refine: A perceptual quality refiner for ai-generated image, 2024. 1
- [30] Zhi Li, Adam Aaron, Ioannis Katsavounidis, Anush K Moorthy, and Manjunath Manohara. Toward a practical perceptual video quality metric. In SMPTE Annual Technical Conference and Exhibition. SPIE, 2016. 3
- [31] Youwei Liang, Junfeng He, Gang Li, Peizhao Li, Arseniy Klimovskiy, Nicholas Carolan, Jiao Sun, Jordi Pont-Tuset, Sarah Young, Feng Yang, et al. Rich human feedback for text-to-image generation. In *Proceedings of the IEEE/CVF Conference on Computer Vision and Pattern Recognition*, pages 19401–19411, 2024. 1, 3
- [32] Zhiqiu Lin, Deepak Pathak, Baiqi Li, Jiayao Li, Xide Xia, Graham Neubig, Pengchuan Zhang, and Deva Ramanan. Evaluating text-to-visual generation with image-to-text generation. *arXiv preprint arXiv:2404.01291*, 2024. 1, 3, 4
- [33] Jie Liu, Gongye Liu, Jiajun Liang, Ziyang Yuan, Xiaokun Liu, Mingwu Zheng, Xiele Wu, Qiulin Wang, Menghan Xia, Xintao Wang, Xiaohong Liu, Fei Yang, Pengfei Wan, Di Zhang, Kun Gai, Yujiu Yang, and Wanli Ouyang. Improving video generation with human feedback, 2025.
- [34] Renjie Liu, Ze Lin, Yutong Cao, Han Hu, Yixuan Wei, Zheng Zhang, Bin Guo, and Jifeng Han. Fastvqa: Efficient video quality assessment with transformers. In *CVPR*, 2022. 3, 7
- [35] Xiaohong Liu, Xiongkuo Min, Guangtao Zhai, Chunyi Li, Tengchuan Kou, Wei Sun, Haoning Wu, Yixuan Gao, Yuqin

- Cao, Zicheng Zhang, et al. Ntire 2024 quality assessment of ai-generated content challenge. In *Proceedings of the IEEE/CVF Conference on Computer Vision and Pattern Recognition*, pages 6337–6362, 2024. 1, 2
- [36] Kenneth Marino, Mohammad Rastegari, Ali Farhadi, and Roozbeh Mottaghi. Ok-vqa: A visual question answering benchmark requiring external knowledge. In *Proceedings of the IEEE/cvf conference on computer vision and pattern recognition*, pages 3195–3204, 2019. 2
- [37] Maria Perez-Ortiz, Aliaksei Mikhailiuk, Emin Zerman, Vedad Hulusic, Giuseppe Valenzise, and Rafał K Mantiuk. From pairwise comparisons and rating to a unified quality scale. *IEEE Transactions on Image Processing*, 29:1139– 1151, 2019. 2
- [38] Tim Salimans, Ian Goodfellow, Wojciech Zaremba, Vicki Cheung, Alec Radford, Xi Chen, and Xi Chen. Improved techniques for training gans. In Advances in neural information processing systems, pages 2234–2242, 2016. 3
- [39] K Seshadrinathan, R Soundararajan, AC Bovik, and LK Cormack. Study of subjective and objective quality assessment of video. *IEEE Transactions on Image Processing*, 19(6): 1427–1441, 2010. 3
- [40] Guangming Sheng, Chi Zhang, Zilingfeng Ye, Xibin Wu, Wang Zhang, Ru Zhang, Yanghua Peng, Haibin Lin, and Chuan Wu. Hybridflow: A flexible and efficient rlhf framework. In *Proceedings of the Twentieth European Conference* on Computer Systems, page 1279–1297. ACM, 2025. 7
- [41] Kuaishou Team. Kling ai. https://klingai.io/, 2024. 4
- [42] Kwai Keye Team, Biao Yang, Bin Wen, Changyi Liu, Chenglong Chu, Chengru Song, Chongling Rao, Chuan Yi, Da Li, Dunju Zang, Fan Yang, Guorui Zhou, Hao Peng, Haojie Ding, Jiaming Huang, Jiangxia Cao, Jiankang Chen, Jingyun Hua, Jin Ouyang, Kaibing Chen, Kaiyu Jiang, Kaiyu Tang, Kun Gai, Shengnan Zhang, Siyang Mao, Sui Huang, Tianke Zhang, Tingting Gao, Wei Chen, Wei Yuan, Xiangyu Wu, Xiao Hu, Xingyu Lu, Yang Zhou, Yi-Fan Zhang, Yiping Yang, Yulong Chen, Zhenhua Wu, Zhenyu Li, Zhixin Ling, Ziming Li, Dehua Ma, Di Xu, Haixuan Gao, Hang Li, Jiawei Guo, Jing Wang, Lejian Ren, Muhao Wei, Qianqian Wang, Qigen Hu, Shiyao Wang, Tao Yu, Xinchen Luo, Yan Li, Yiming Liang, Yuhang Hu, Zeyi Lu, Zhuoran Yang, and Zixing Zhang. Kwai keye-vl technical report, 2025. 6
- [43] Techreport. Ai image generator market statistics in 2024. *Techreport*, 2024. Accessed: 2024-10-14. 1
- [44] Jianyi Wang, Kelvin C. K. Chan, and Chen Change Loy. Exploring clip for assessing the look and feel of images, 2022.
- [45] Jiarui Wang, Huiyu Duan, Jing Liu, Shi Chen, Xiongkuo Min, and Guangtao Zhai. Aigciqa2023: A large-scale image quality assessment database for ai generated images: from the perspectives of quality, authenticity and correspondence. In CAAI International Conference on Artificial Intelligence, pages 46–57. Springer, 2023. 1, 3
- [46] Yibin Wang, Yuhang Zang, Hao Li, Cheng Jin, and Jiaqi Wang. Unified reward model for multimodal understanding and generation, 2025. 7

- [47] Haoning Wu, Erli Zhang, Liang Liao, Chaofeng Chen, Jingwen Hou, Annan Wang, Wenxiu Sun, Qiong Yan, and Weisi Lin. Exploring video quality assessment on user generated contents from aesthetic and technical perspectives, 2023. 7
- [48] Haoning Wu, Zicheng Zhang, Erli Zhang, Chaofeng Chen, Liang Liao, Annan Wang, Chunyi Li, Wenxiu Sun, Qiong Yan, Guangtao Zhai, and Weisi Lin. Q-bench: A benchmark for general-purpose foundation models on low-level vision. In *ICLR*, pages 1–13, 2023. 1
- [49] Haoning Wu, Zicheng Zhang, Erli Zhang, Chaofeng Chen, Liang Liao, Annan Wang, Kaixin Xu, Chunyi Li, Jingwen Hou, Guangtao Zhai, et al. Q-Instruct: Improving low-level visual abilities for multi-modality foundation models. *IEEE CVPR*, pages 1–16, 2024.
- [50] Haoning Wu, Zicheng Zhang, Weixia Zhang, Chaofeng Chen, Liang Liao, Chunyi Li, Yixuan Gao, Annan Wang, Erli Zhang, Wenxiu Sun, Qiong Yan, Xiongkuo Min, Guangtao Zhai, and Weisi Lin. Q-align: Teaching lmms for visual scoring via discrete text-defined levels. In *ICML2024*, 2024. 3, 4, 5, 7
- [51] Xiaoshi Wu, Yiming Hao, Keqiang Sun, Yixiong Chen, Feng Zhu, Rui Zhao, and Hongsheng Li. Human preference score v2: A solid benchmark for evaluating human preferences of text-to-image synthesis. arXiv preprint arXiv:2306.09341, 2023. 1, 3
- [52] Xiaoshi Wu, Keqiang Sun, Feng Zhu, Rui Zhao, and Hongsheng Li. Better aligning text-to-image models with human preference. *CoRR*, abs/2303.14420, 2023. 1
- [53] Jiazheng Xu, Xiao Liu, Yuchen Wu, Yuxuan Tong, Qinkai Li, Ming Ding, Jie Tang, and Yuxiao Dong. ImageReward: Learning and evaluating human preferences for texto-image generation. *CoRR*, abs/2304.05977, 2023. 1, 3
- [54] Jiazheng Xu, Yu Huang, Jiale Cheng, Yuanming Yang, Jiajun Xu, Yuan Wang, Wenbo Duan, Shen Yang, Qunlin Jin, Shurun Li, Jiayan Teng, Zhuoyi Yang, Wendi Zheng, Xiao Liu, Ming Ding, Xiaohan Zhang, Xiaotao Gu, Shiyu Huang, Minlie Huang, Jie Tang, and Yuxiao Dong. Visionreward: Fine-grained multi-dimensional human preference learning for image and video generation, 2025. 7
- [55] Jiquan Yuan, Fanyi Yang, Jihe Li, Xinyan Cao, Jinming Che, Jinlong Lin, and Xixin Cao. Pku-aigiqa-4k: A perceptual quality assessment database for both text-to-image and image-to-image ai-generated images. arXiv preprint arXiv:2404.18409, 2024. 1, 3
- [56] Emin Zerman, Vedad Hulusic, Giuseppe Valenzise, Rafał K Mantiuk, and Frédéric Dufaux. The relation between mos and pairwise comparisons and the importance of crosscontent comparisons. *Electronic Imaging*, 30:1–6, 2018. 2
- [57] Guoli Zhai, Weisi Lin, and Hui Shen. Video Quality Assessment. Springer, 2016. 3
- [58] Richard Zhang, Phillip Isola, Alexei A. Efros, Eli Shechtman, and Oliver Wang. The unreasonable effectiveness of deep features as a perceptual metric. In *IEEE CVPR*, pages 586–595, 2018. 3
- [59] Xinlu Zhang, Yujie Lu, Weizhi Wang, An Yan, Jun Yan, Lianke Qin, Heng Wang, Xifeng Yan, William Yang Wang, and Linda Ruth Petzold. Gpt-4v (ision) as a general-

- ist evaluator for vision-language tasks. arXiv preprint arXiv:2311.01361, 2023. 1, 3
- [60] Zicheng Zhang, Ziheng Jia, Haoning Wu, Chunyi Li, Zijian Chen, Yingjie Zhou, Wei Sun, Xiaohong Liu, Xiongkuo Min, Weisi Lin, et al. Q-bench-video: Benchmarking the video quality understanding of lmms. arXiv preprint arXiv:2409.20063, 2024. 1
- [61] Zicheng Zhang, Haoning Wu, Zhongpeng Ji, Chunyi Li, Erli Zhang, Wei Sun, Xiaohong Liu, Xiongkuo Min, Fengyu Sun, Shangling Jui, et al. Q-boost: On visual quality assessment ability of low-level multi-modality foundation models. In 2024 IEEE International Conference on Multimedia and Expo Workshops (ICMEW), pages 1–6. IEEE, 2024. 1, 5
- [62] Zicheng Zhang, Haoning Wu, Chunyi Li, Yingjie Zhou, Wei Sun, Xiongkuo Min, Zijian Chen, Xiaohong Liu, Weisi Lin, and Guangtao Zhai. A-bench: Are lmms masters at evaluating ai-generated images? arXiv preprint arXiv:2406.03070, 2024. 1, 2
- [63] Zicheng Zhang, Haoning Wu, Erli Zhang, Guangtao Zhai, and Weisi Lin. Q-bench+: A benchmark for multi-modal foundation models on low-level vision from single images to pairs. *arXiv preprint arXiv:2402.07116*, 2024. 1
- [64] Zicheng Zhang, Haoning Wu, Yingjie Zhou, Chunyi Li, Wei Sun, Chaofeng Chen, Xiongkuo Min, Xiaohong Liu, Weisi Lin, and Guangtao Zhai. Lmm-pcqa: Assisting point cloud quality assessment with lmm. In *Proceedings of the 32nd ACM International Conference on Multimedia*, pages 7783–7792, 2024. 1
- [65] Zicheng Zhang, Yingjie Zhou, Chunyi Li, Baixuan Zhao, Xiaohong Liu, and Guangtao Zhai. Quality assessment in the era of large models: A survey. arXiv preprint arXiv:2409.00031, 2024. 1, 2

Q-Save: Towards Scoring and Attribution for Generated Video Evaluation

Supplementary Material

A. Dataset Details

A.1. Dataset Construction Details

In this section, we mainly talk about the details of prompts collection.

Prompts Collection Table 4 presents the distribution of prompts across five major entity categories—Human, Animal, Plant, Object, and Virtual Subject-based on the number of times each category appears within a single prompt. The quantity ranges are divided into five bins: 1-3, 4-6, 7-9, 10 or more, and unknown (cases where quantity could not be determined explicitly). Most prompts involving Humans and Objects appear in the 1-3 range, reflecting a common design bias toward fewer instances of these entities. In contrast, categories like Animals and Objects exhibit higher frequencies in the "10 or more" range, likely due to prompts involving groups, crowds, or complex scenes. Notably, the "unknown" bin is most prominent for Plants and Objects, indicating frequent use of implicit or abstract descriptions in those categories. This distribution analysis highlights the variation in prompt complexity and provides insights into how different entity types are quantitatively represented in the dataset.

Table 6 presents a detailed breakdown of prompt elements classified into two major categories: Scene and Subject. Each main category is further divided into several subcategories and sub-subcategories to reflect the diversity and granularity of the prompts. For example, the **Scene** category includes human-centric, natural, and virtual scenes, with further distinctions such as indoor, outdoor, and abstract environments. Similarly, the Subject category encompasses humans, animals, plants, objects, and abstract virtual entities, capturing both physical and conceptual entities. The count column reflects the number of prompt instances associated with each (sub)category, indicating areas with higher representation, such as human subjects (253 instances) and object-related prompts (396 instances). This hierarchical structure helps to systematically analyze prompt diversity and distribution.

Table 5 provides a comprehensive categorization of prompt-related elements that influence the expressive style and visual dynamics of generated content. The table is divided into three major sections: **Style and Atmosphere**, **Lens Parameters**, and **Spatial Relationships**. The Style and Atmosphere category includes both emotional tones (e.g., sad, humorous, suspenseful) and artistic styles (e.g., anime, watercolor, pixel art), along with other modifiers such as lighting and color intensifiers. The Lens Param-

Table 4. Distribution of Prompts by Entity Category and Quantity Range. Each cell shows the number of prompts containing a specific category (e.g., Human, Animal) within the indicated quantity range.

Categary			Quan	tity range	
Categary	1-3	4-6	7-9	10 or more	unknown
Human	278	25	20	8	7
Animal	161	49	18	41	15
Plant	34	16	15	5	76
Object	434	24	19	65	213
Virtual Subject	82	45	14	18	13

eters section captures cinematic techniques used in visual storytelling, such as camera movements (e.g., tilt, pan, push/pull), shooting types (e.g., long shot, close-up), and temporal effects (e.g., slow motion, time-lapse). Finally, the Spatial Relationships category records directional placements (e.g., up, down, front, back), indicating how entities are arranged or oriented in the scene. This taxonomy helps to reveal the diversity and richness of descriptive control available in prompt design for multimodal generation systems.

Subjective Annotation Protocol. We construct our dataset with 10,000 videos, incorporating rigorous subjective evaluation protocols to ensure annotation quality. Each instance in the training and test sets is rated by at least 3 and 12 individuals, respectively. For low-quality instances (i.e., those with a mean opinion score (MOS) below 4), we further collect fine-grained **attribution annotations** to explain the source of quality degradation.

To ensure rater reliability and diversity, we recruit annotators from a wide age range (18–52) and various professional backgrounds. Each rater is limited to labeling a maximum of 30 videos per session, followed by a mandatory 30-minute break to prevent fatigue. In particularly high-quality cases (i.e., perfect-score videos), the annotations are first provided by 12 individuals and subsequently reviewed and adjusted by a group of 5 domain experts.

Given that we additionally perform time-consuming attribution annotation for all low-quality videos, following the ITU-recommended standard of 15 raters per instance would be impractical in terms of time and cost. To maintain the dataset's scale, which is essential for training large multimodal models under scaling laws, we adopt a *Sample and Scrutinize* strategy: a subset of 160 videos is annotated by all raters, with expert-generated ground-truth annotations

Table 5. Prompt Elements Categorized by Style, Lens Parameters, and Spatial Relationships

Category	Subcategory	Count		
	Atmosphere	109		
	Sad	16		
	Romantic	13		
	Calm/Tranquil	19		
	Other	2		
	Fantasy	11		
	Lively	4		
	Warm	4		
	Suspenseful	12		
	serious	3		
	Humorous/Cheerful	25		
	Style	139		
Style and atmosphere	3D-cartoon	17		
Styte and atmosphere	80s vapor wave	6		
	Master	7		
	Anime	29		
	Black & White	22		
	Claymation	1		
	Moody	6		
	Pixel art	5		
	Realistic	27		
	Sci-fi art	9		
	Stickers	2		
	Watercolor	8		
	Others	133		
	Composition			
	Light and shadow	67		
	intensifiers	31		
	color	34		
	Scene	113		
	Panoramic/Wide angle	35		
	Close-up	29		
	Long shot	22		
	Medium shot/Close shot	27		
	Lens movement	168		
	Tilt	30		
	Vertical	21		
	Roll	2		
	Surround	23		
	Pan	34		
	Other	8		
Lens parameters	Horizontal	26		
Lens parameters	Push/Pull	24		
	Shooting techniques	105		
	background blur/depth of field			
	zoom/scaling	22		
	high-speed photography	15		
	tracking	25		
	slow motion	28		
	time-lapse	35		
	viewing angle	47		
	overhead/aerial photography	25		
	Others	4		
	looking up	18		
		273		
	Spatial relationships			
	U p	146		
Spatial relationships	Ūp Down	146 40		
Spatial relationships	Up Down Right	146 40 24		
Spatial relationships	Up Down Right Left	146 40 24 23		
Spatial relationships	Up Down Right	146 40 24		

provided by 10 specialists. Based on the agreement with these ground truths, we identify and exclude the 6 least accurate annotators from the final dataset to ensure labeling quality. The distribution of annotation variance is illustrated in Fig. 9, where the majority of instances exhibit a variance below 0.3, demonstrating strong inter-rater consistency.

Reinforcement Learning Dataset. We selected 200 high-quality prompts from various datasets. These prompts align with our prompt collection principles in terms of difficulty and category distribution, while being distinct from those in our SFT dataset. We employed six models entirely different from those used for the SFT dataset:

Table 6. Categorized Statistics of Prompt Elements Across Scene and Subject Types

Category	Subcategory	Count
	Human scenes	136
	Indoor	
	Outdoor	52
	Famous humanities classics	35
	Virtual Scene	102
Scene	Abstract Scene	<u>18</u> -
Scene	Science Fiction Scene	29
	Dream Scene	30
	Virtual and Real Interweaving	15
	Well-known Virtual Scene	10
	Natural Scene	146
	Air	47
	Land	51
	Water	51
	Famous Natural Attractions	26
	Human	253
	Wear	40
	Age/Era	33
	Ethnicity	28
	Physical Characteristics	34
	Number	31
	Gender	41
	Famous Person	8
	Occupation	38
	Animals/Microorganisms	154
	Air	49
	Land	51
	Water	52
Subject	Microscopic/internal	2
J	Plant	63
	Land	32
	Water	31
	Object	396 -
	Work/Study Objects	
	Others	104
	Food	62
	Cultural/Entertainment Objects	46
	Travel	37
	Clothing	32
	Sports/Health	33 43
	Housing Virtual Subject/A betract Concept	227
	Virtual Subject/Abstract Concept	221 -
	Abstract symbol Abstract symbol (text)	29 117
	Virtual creature	29
	Virtual Creature Virtual Objects	30
	Well-known virtual image	22
		44

Kling2.1, HailuoAI, Veo3, Seedance-1.0-lite, Wanx-2.1-plus, and PixverseV4. The annotation standards and processes for this dataset are identical to those of the SFT dataset.

A.2. The Performance of Generative Model

Model performance in different categories Figure 3 presents four radar charts visualizing the performance of four different models across various semantic categories under multiple evaluation dimensions. Each radar chart corresponds to a specific evaluation aspect (e.g., visual quality, motion quality, alignment, or overall quality), with axes representing performance scores in specific content categories such as Humans, Animals, Objects, and Virtual Subjects.

The radar plots reveal that **Veo2** achieves more balanced and consistent performance across all categories, particularly excelling in Object and Virtual Subject scenarios. In contrast, **Kling2.0** shows strong alignment and visual qual-

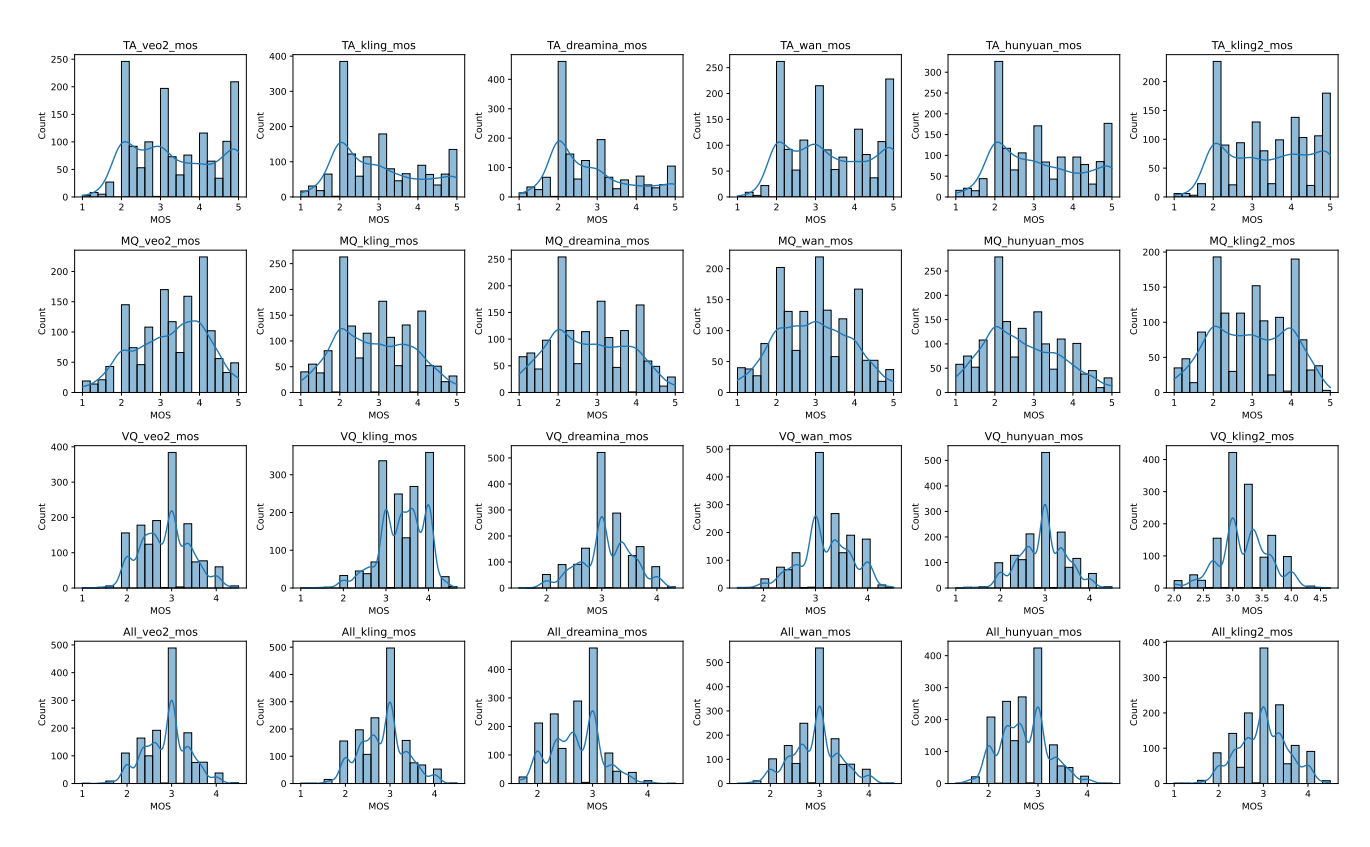


Figure 5. Distribution of Mean Opinion Scores (MOS) across six generative models (Veo2, Kling, Kling2.0, Hunyuan, Dreamina, Wan), evaluated along four quality dimensions: Text Alignment (TA), Motion Quality (MQ), Visual Quality (VQ), and Overall Quality (All). Each subplot represents a model-dimension pair, with MOS scores (1–5) on the x-axis and frequency counts (0–500) on the y-axis. Blue bars denote histogram counts, while overlaid curves represent smoothed kernel density estimates.

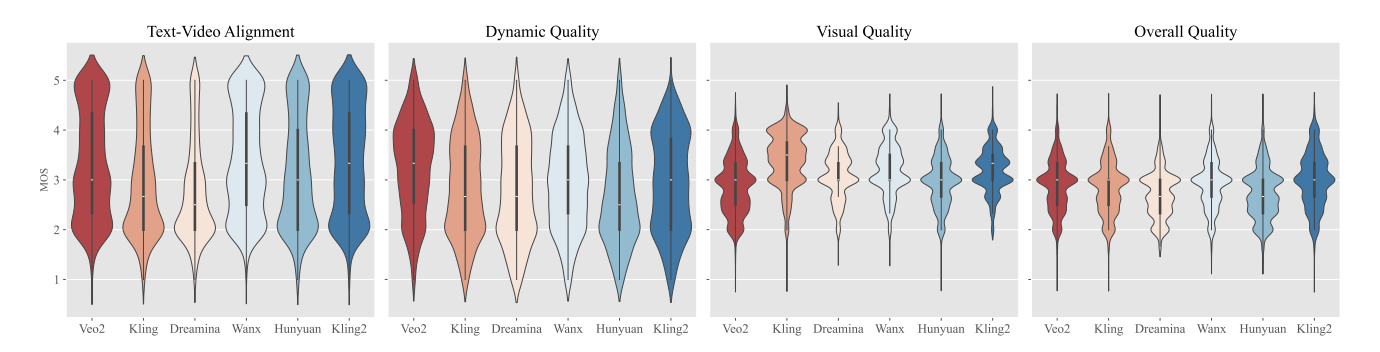


Figure 6. MOS distributions for the visual quality, dynamic quality, text-video alignment and overall of generated videos in the Q-Save dataset respectively

ity in Human-centric content, but underperforms in categories involving abstract or non-human subjects. **Dreamina** exhibits high variance, with excellent performance in motion quality but lower scores in categories requiring semantic consistency. **Hunyuan** demonstrates moderate yet stable scores across most categories, suggesting a trade-off strategy in model design.

MOS Distribution Analysis. Figure 5 visualizes the distribution of Mean Opinion Scores (MOS) for six state-of-the-art generative models—Veo2, Kling, Kling2.0, Hunyuan, Dreamina, and Wan—evaluated across four key quality dimensions: Text Alignment (TA), Motion Quality (MQ), Visual Quality (VQ), and Overall Quality (All). Each subplot in the figure corresponds to a specific model-dimension pair, with histogram bars indicating frequency



Figure 7. Radar charts comparing the performance of four models across different semantic categories under four evaluation dimensions.

counts and overlaid curves representing smoothed density estimates. These visualizations provide insights into how different models perform across evaluation axes and semantic domains.

Across models, several distinctive distributional patterns emerge. Veo2 demonstrates strong performance in TA, with scores clustering near 4, while its MQ scores show a bimodal distribution (peaks at MOS 3 and 4.5), suggesting instability in motion generation. Kling2.0 consistently achieves high VQ ratings, with over 80% of samples rated 4 or higher, but exhibits left-skewed TA scores (median = 3.5), indicating potential issues in text-video alignment. Hunyuan presents a notable anomaly in TA, with a dual-peaked distribution centered around MOS 2.5 and 4—this likely reflects stylistic diversity that polarized raters. In contrast, Wan underperforms across all dimensions, with left-skewed distributions and overall MOS medians between 2.8 and 3.2, suggesting limited robustness in both content generation and coherence.

From a dimension-centric perspective, the TA scores

are generally right-skewed (median = 4.1), suggesting that most models are relatively successful in capturing textual alignment, though Hunyuan displays higher variance ($\sigma=1.2$), pointing to inconsistency. Motion Quality exhibits the greatest inter-model variability: Veo2 shows a bimodal shape, Dreamina's distribution is nearly uniform (entropy = 1.6), and Kling shows a near-normal shape with moderate variance ($\sigma=0.7$). Visual Quality is the most predictive of user-perceived quality, with a strong positive correlation with overall scores (Pearson's r=0.89, p<0.001). Notably, Kling2.0 achieves the most stable overall ratings (95% confidence interval [4.1, 4.3]), while Dreamina yields the widest spread (IQR = 1.8), suggesting diverse output quality.

Finally, several statistical irregularities are worth noting. Wan's MQ distribution shows a floor effect, with nearly 30% of ratings falling below MOS 2, indicating recurrent motion artifacts. Conversely, Veo2's VQ distribution shows a ceiling effect, with 15% of samples receiving a perfect score of 5, highlighting superior visual rendering. Addi-

tionally, Kling's TA ratings appear truncated below MOS 2, which may point to filtering biases in sample selection or annotation. These findings collectively reveal both the strengths and limitations of current generative models and motivate further efforts toward dimension-specific evaluation and rater calibration.

B. More experimental details

B.1. Reward model baselines

Q-ALIGN is a human-emulating syllabus for training large multi-modality models (LMMs) in visual scoring. It converts mean opinion scores (MOS) into five text-defined rating levels (excellent/good/fair/poor/bad) for training, and infers scores via softmax pooling and weighted average of level probabilities during inference. By unifying image quality assessment (IQA), image aesthetic assessment (IAA), and video quality assessment (VQA) under one LMM structure, it achieves state-of-the-art performance with high data efficiency and strong out-of-distribution generalization.

DOVER is proposed based on the View Decomposition strategy, with two branches dedicated to aesthetic and technical perspectives respectively. It uses specific inputs, regularization strategies and pretraining to match each perspective's characteristics, and adopts subjectively-inspired fusion of dual-branch predictions for overall quality evaluation.

VisionReward introduces a fine-grained, multidimensional evaluation framework for both image and video domains. It trains separate reward models tailored to human preferences collected through carefully curated datasets, offering strong baselines for visual content

VideoScore-v2 focuses on assessing video generation quality. It is trained on the VideoFeedback dataset comprising human-annotated scores over 37.6K videos, each evaluated across multiple aspects including fidelity, consistency, and alignment.

VideoReward offers a multi-dimensional assessment for video generation tasks. It is trained on a large-scale 182K dataset of human-labeled comparisons collected from outputs of 12 video generation models, providing strong performance on complex video benchmarks.

UnifiedReward serves as our base architecture. It leverages multi-task learning across diverse image and video generation and understanding datasets. By unifying multi-modal reward tasks into a single framework, UnifiedReward demonstrates mutual enhancement effects and establishes a solid baseline for holistic visual reward modeling.

AIGVE-MACS is a unified evaluation framework for AIgenerated videos. It is fine-tuned on the large-scale humanannotated AIGVE-BENCH 2 dataset, integrating tokenwise weighted loss and dynamic frame sampling strategy to fully leverage the generative capabilities of Vision-Language Models (VLMs). By jointly producing aspectwise numerical scores and multi-aspect natural language comments, it achieves strong alignment with human judgments and sets a new paradigm for interpretable and comprehensive AI-generated video evaluation.

VIDEOPHY-2 is an action-centric benchmark for evaluating physical commonsense in video generation. It curates 197 diverse real-world actions, generates 3940 detailed prompts (including dense upsampled versions), and constructs a hard subset for rigorous testing. Through human evaluation on semantic adherence, physical commonsense, and fine-grained physical rule compliance, it exposes model shortcomings, especially in conservation laws. Complemented by the VIDEOPHY-2-AUTOEVAL automatic evaluator (finetuned on 50K human annotations), it provides a scalable, reliable framework for guiding physically-grounded video generation research.

B.2. Evaluation benchmarks

Since different benchmarks define varying dimensions and scoring scales, we align them with the three evaluation dimensions of **Q-Save** (visual quality, text alignment, and physical consistency) and, where necessary, rescale their ground-truth scores.

VideoGenReward Bench. This is a pairwise preference benchmark containing 4,691 videos, forming 25,234 video pairs. It evaluates three dimensions—visual quality (VQ), text alignment (TA), and motion quality (MQ)—and also provides an *Overall* preference label indicating which video is better overall. For the *Overall* preference, we use the mean of all available dimension scores from Q-Save or the baseline method (if the baseline only has one quality score output, then that score is used directly).

T2VQA-DB. Originally a human-annotated video quality dataset with 10,000 videos, each labeled with a single quality score in the range [1,100]. We sample 2,000 videos and construct 1,822 pairs by comparing human-annotated scores. Since the dataset provides only one dimension (the final score), we predict preference by averaging all dimension scores from Q-Save or the baseline method (if the baseline only has one quality score output, then that score is used directly).

GenAI-Bench. This is a multimodal generation benchmark designed to assess how well models align with human preferences across image and video generation tasks. We adopt its video generation subsets for evaluating generative reward performance.

VideoPhy2-test. This benchmark contains 3,396 videos with two dimensions, SA: *semantic adherence* and PC: *physical consistency*. These map perfectly to Q-Save's second and third dimensions. For baselines lacking one of the dimensions (e.g., VideoReward, which provides VQ, TA, MQ but no physical consistency), we skip the missing dimension. The scoring scale is {1,2,3,4,5}, so no rescaling is required.

VIDEOSCORE-BENCH-V2. This is an point-score benchmark constructed from 500 held-out videos from the VIDEOFEEDBACK2 dataset. It evaluates videos across three core dimensions: visual quality, text alignment, and physical/common-sense consistency. The benchmark uses integer scores in the range [1,5] and adopts multiple evaluation metrics, including Accuracy (exact match between model and human scores), Relaxed Accuracy (allowing a maximum 1-point difference from human scores), and PLCC (Pearson Linear Correlation Coefficient) to measure the consistency between model predictions and human annotations.

C. Visualization Results

Using MOS as the ground truth, we summarize the performance of evaluation methods across three dimensions (each with three examples) based on Figures 8, 9, 10 and 11, . In short, Q-Save shows comprehensive adaptability across dimensions, confirming its value as a unified text-to-vision evaluation framework.

D. Data Statement

Considering the large scale of the dataset and the complexity of the model, we are actively organizing and refining the content to ensure its quality and usability. We solemnly pledge to release the **Q-Save** dataset in the near future, ensuring a comprehensive and systematic open-sourcing process that effectively supports community development. **Furthermore, we confirm that the dataset has successfully passed ethical review, affirming our commitment to responsible AI practices.** Alongside the dataset, we will also release **Q-Save** and provide continuous updates, ensuring the model remains aligned with the rapid advancements in generative AI.

E. Broader Impact

Unifying Scoring and Attribution. We propose a novel model that not only predicts quality scores but also provides human-interpretable attribution, bridging quantitative evaluation with qualitative reasoning and promoting transparency in generative content assessment.

A Dual-Purpose Evaluation Benchmark. We release a large-scale dataset with both MOS-style scores and fine-

grained attribution labels, enabling comprehensive evaluation and diagnostic analysis through a unified, dual-supervision framework.

Enabling Informed Model Development. Our model and dataset support the design and refinement of generative systems. Scoring ensures quality control, while attribution enables targeted improvements, together advancing safer and more aligned AI deployment.

F. Limitations

Subjectivity in Attribution. Despite expert verification, attribution remains inherently subjective. Visual flaws or semantic errors may be interpreted differently across users and cultures.

Annotation Cost and Scalability. High-quality scoring and attribution require expert labor, limiting scalability. Reducing annotation cost through automation while maintaining quality is a key challenge.

Coverage of Attribution Categories. Our current schema covers core dimensions (e.g., text alignment, motion quality), but may miss subtler issues like aesthetic intent, suggesting space for future extension.

The egg slipped from a hand and hit the floor with a heavy thud, instantly breaking apart. The egg yolk splattered and the shell shattered. The video was shot in slow motion, capturing the entire breaking process.



At sunset, the golden sand dunes in the desert shine brightly under the rays of the setting sun. The camera moves from left to right.



In the square, an old man is writing characters with a big brush dipped in water. He writes the words "Spring warmth brings harmony and prosperity to the household".



Figure 8. Visualization comparison results of text-video alignment.

A cluster of aquatic plants sways gently with the current at the lake bottom, their emerald green foliage resembling an underwater forest.



An eagle soars through the sky, the camera zooms in to highlight its sharp eyes. Deep within the eagle's gaze, the reflection of five or six rabbits can be seen frantically running away across the prairie.



A waterfall composed of various mathematical symbols, cascading down.



Figure 9. Visualization comparison results of visual quality.

A muscular white athlete is lifting a barbell.



A boy and a girl are catching insects. Three bugs are hopping around on the ground, in a 3D cartoon style.



A young man wearing jeans accidentally slipped while descending the stairs. The camera tilted downward, capturing the moment he lost his balance and slid down the stairs, eventually coming to a stop at the bottom.



Figure 10. Visualization comparison results of dynamic quality.

A video is generated showing an ancient person wielding a brush, writing the large characters \"叶公好龙\". The calligraphy is in very large font.



Ground Truth: Visual Quality - 3.08, Dynamic Quality: 2.42, Text-Video Consistency: 2.08

VideoScore-v2

<think>

Visual Quality Analysis:

Looking at the frames, I observe that the visual quality is excellent overall. The frames show crisp details of the calligrapher's hands, the brush, the ink strokes, and the character on the paper. Lighting remains steady and cinematic, with convincing depth of field that keeps the subject in sharp focus while background elements stay softly rendered. There are no noticeable artifacts or distortions, and motion remains smooth across the sequence. The camera work is stable and well composed, contributing to a polished look. Overall, Visual Quality aligns with top-tier production values. Text-to-Video Alignment Analysis:

The scene adheres closely to the prompt: an ancient-looking person wielding a brush, actively writing large characters on a vertical surface, with the calligraphy rendered in a very large font. The sequence accurately captures the essential actions described, including the grip, posture, and progression of stroke application. The composition and scale emphasize the intended emphasis on the characters, resulting in strong alignment between the video content and the prompt. Minor stylistic embellishments do not detract from the core alignment.

Physical/Common-sense Consistency Analysis:

The motion and interactions reflect authentic calligraphic technique. Hand positioning and brush handling appear natural, with deliberate, controlled strokes that correspond to traditional Chinese calligraphic practice. The dynamics are consistent with real-world physics, and there are no evident inconsistencies in tool interaction or body movement. The depiction maintains plausible proportions and timing throughout, indicating a high degree of physical authenticity. In summary, the video demonstrates excellent Visual Quality, strong Text-to-Video Alignment, and high Physical Consistency, corresponding to scores of 5 for all three dimensions.

</think>

- (1) visual quality clarity, smoothness, artifacts: 5
- (2) text-to-video alignment fidelity to the prompt: 5
- (3) physical/common-sense consistency naturalness and physics plausibility: 5

Q-Save

Text-Video Consistency:

<think>The video content is inconsistent with the prompt. The prompt requested the generation of a video showing the writing of the large characters '叶公好龙' (Yè Gōng Hǎo Lóng), but the video only shows the character '礼' (Lǐ) being written.</think>Poor

Dynamic Quality:

<think> The motion of the person writing the character '龙' (dragon) with a brush is unnatural and unreasonable. The brushstrokes appear stiff, and the way the brush moves across the paper does not conform to the fluid, continuous actions of real calligraphy, lacking the rhythm and pressure variations (lifting, pressing, pausing) characteristic of brushwork. The overall impression is more like a simple animation effect rather than authentic writing.

Visual Quality:

<think>The overall clarity of the video is low, making the image appear somewhat blurry and lacking sharpness. This is particularly noticeable in the details of the brushstrokes, the texture of the paper, and the details of the person's hands, which are not clearly defined.

Figure 11. Visualization comparison results of CoT results.